Received: 22 August 2019 | Revised: 10 November 2019 | Accepted: 3 December 2019

DOI: 10.1111/cmi.13151

SPECIAL ISSUE - RESEARCH ARTICLE

WILEY

Components of the endocytic and recycling trafficking pathways interfere with the integrity of the *Legionella*-containing vacuole

Ila S. Anand | Wonyoung Choi | Ralph R. Isberg

Department of Molecular Biology and Microbiology, Tufts University School of Medicine, Boston, Massachusetts

Correspondence
Ralph R. Isberg, Tufts University School of Medicine, 150 Harrison Ave., Boston, MA 02111.
Email: ralph.isberg@tufts.edu

Funding information
Howard Hughes Medical Institute; National Institute of Allergy and Infectious Diseases, Grant/Award Number: R01AI113211; National Institute of General Medical Sciences, Grant/Award Number: T32GM07310; NIH

Abstract

Legionella pneumophila requires the Dot/Icm translocation system to replicate in a vacuolar compartment within host cells. Strains lacking the translocated substrate *SdhA* form a permeable vacuole during residence in the host cell, exposing bacteria to the host cytoplasm. In primary macrophages, mutants are defective for intracellular growth, with a pyroptotic cell death response mounted due to bacterial exposure to the cytosol. To understand how *SdhA* maintains vacuole integrity during intracellular growth, we performed high-throughput RNAi screens against host membrane trafficking genes to identify factors that antagonise vacuole integrity in the absence of *SdhA*. Depletion of host proteins involved in endocytic uptake and recycling resulted in enhanced intracellular growth and lower levels of permeable vacuoles surrounding the Δ*sdhA* mutant. Of interest were three different Rab GTPases involved in these processes: Rab11b, Rab8b and Rab5 isoforms, that when depleted resulted in enhanced vacuole integrity surrounding the *sdhA* mutant. Proteins regulated by these Rabs are responsible for interfering with proper vacuole membrane maintenance, as depletion of the downstream effectors EEA1, Rab11FIP1, or VAMP3 rescued vacuole integrity and intracellular growth of the *sdhA* mutant. To test the model that specific vesicular components associated with these effectors could act to destabilise the replication vacuole, EEA1 and Rab11FIP1 showed increased density about the *sdhA* mutant vacuole compared with the wild type (WT) vacuole. Depletion of Rab5 isoforms or Rab11b reduced this aberrant redistribution. These findings are consistent with *SdhA* interfering with both endocytic and recycling membrane trafficking events that act to destabilise vacuole integrity during infection.

KEYWORDS

intracellular growth, *Legionella*, Rab proteins, RNAi, vesicle trafficking

1 | INTRODUCTION

Legionella pneumophila is a fastidious Gram-negative bacterium that grows intracellularly in both fresh water amoebae and human alveolar macrophages (Isberg, O'Connor, & Heidtman, 2009). Disease in humans is initiated after inhalation of aerosolised water particles contaminated with the bacterium (Cunha, Burillo, & Bouza, 2016). Upon entry into the lungs, *L. pneumophila* is internalised by alveolar

macrophages with its most severe manifestation being Legionnaires' disease pneumonia (Horwitz & Maxfield, 1984; Horwitz & Silverstein, 1980). In both amoebae and macrophages, the ability of *L. pneumophila* to replicate intracellularly is dependent on the Icm/Dot type IV secretion system (T4SS) (Segal, Feldman, & Zusman, 2005). This complex introduces more than 300 translocated substrates into the host cell cytosol, which promote establishment of the *Legionella*-containing vacuole (LCV) and exert a variety of regulatory controls on the host cell (Asrat, de Jesus, Hempstead, Ramabhadran, & Isberg, 2014; Burstein et al., 2016).

Establishment and maintenance of LCV membrane integrity are essential for protection of *L. pneumophila* from innate immune cytosolic sensing (Creasey & Isberg, 2014; Liu et al., 2018). The inability of a bacterial mutant to properly form the LCV or maintain its integrity results in a severe intracellular growth defect and pathogen clearance (Creasey & Isberg, 2012; Wiater, Dunn, Maxfield, & Shuman, 1998). The identification of the Icm/Dot-translocated substrate *SdhA* has greatly contributed to our understanding of the consequences of failure to properly maintain pathogen replication vacuoles (Laguna, Creasey, Li, Valtz, & Isberg, 2006). In the absence of *SdhA*, the LCV becomes disrupted and *L. pneumophila* is detected in the cytoplasm of the infected macrophage (Creasey & Isberg, 2012; Laguna et al., 2006). Bacteria exposed in this fashion to the cytosol are susceptible to recruitment of the interferon-regulated guanylate-binding proteins (GBP) family of anti-microbial proteins, resulting in leakage of lipopolysaccharide (LPS) and activation of caspase-11 (Creasey & Isberg, 2012; Liu et al., 2018; Piro et al., 2017). As a consequence, gasdermin D is activated and pyroptotic cell death ensues (Aachoui et al., 2013; Pilla et al., 2014; Shi et al., 2015).

We previously demonstrated that mutations that removed the bacterial phospholipase PlaA rescued the defect in vacuole integrity observed with the Δ*sdhA* mutant, resulting in increased numbers of intracellular bacteria, thus demonstrating that PlaA promotes vacuole disruption (Creasey & Isberg, 2012). PlaA bears homology to the translocated phospholipase SseJ from *Salmonella* typhimurium, which is also involved in vacuole disruption in the absence of another *Salmonella* translocated substrate, SifA (Akoh, Lee, Liaw, Huang, & Shaw, 2004; Flieger, Neumeister, & Cianciotto, 2002; Ruiz-Albert et al., 2002). During infection, SifA binds host factor SKIP and sequesters Rab9 to prevent delivery of M6PR cargo to the vacuole (McGourty et al., 2012). The resemblance between *SdhA*/PlaA and SifA/SseJ suggests that *SdhA* may regulate host membrane trafficking events to maintain LCV integrity.

In addition to *Salmonella*, other pathogens have been reported to interface with host membrane trafficking pathway as a strategy for maintaining vacuolar integrity. The *Chlamydia* protein IncD was shown to recruit the host CERT-VAP complex to the inclusion and enable acquisition of host lipids that are essential for inclusion membrane stability (Derre, Swiss, & Agaisse, 2011). Recently, the *Shigella* vacuole has been reported to interact with endocytic Rab5-positive vesicles and recycling Rab11-positive vesicles to facilitate vacuole membrane rupture, indicating that vacuole integrity can be disrupted by interfacing with appropriate cellular compartments (Mellouk et al., 2014; Weiner et al., 2016). In this study, we determine if the disruption of LCV integrity that results from loss of *L. pneumophila SdhA* function can be attributed to a subset of host membrane trafficking pathways. Using high-throughput screening strategies, we identified specific endocytic and recycling Rab GTPase isoforms and their downstream effectors as playing a role in vacuole disruption resulting from challenge with the *ΔsdhA* strain. The similarity between *Legionella* and *Shigella* interactions with a common endocytic-recycling pathway provides an example of how a host process can either promote or interfere with pathogen replication, depending on the strategy used for intracellular growth.

2 | RESULTS

2.1 | Identification of host proteins that contribute to disruption of *L. pneumophila ΔsdhA* intracellular growth

To identify host membrane trafficking pathways that interfere with growth of the *L. pneumophila ΔsdhA* mutant, we carried out a screen using an siRNA library targeting genes known to participate in membrane trafficking and remodelling. RAW 264.7 macrophages are known to be defective in the activation of pyroptosis and clearance in response to cytoplasmic exposure of *L. pneumophila* pattern recognition molecules, so growth of the mutant could be followed without premature host cell death downstream of cytoplasmic bacterial exposure (Pelegrin, Barroso-Gutierrez, & Surprenant, 2008). This allowed subtle differences in intracellular growth to be detected. RAW 264.7 macrophages were seeded in 96-well plates and transfected with an arrayed siRNA library against 112 mouse genes involved in membrane trafficking (Tables S1 and S2). Each well contained 4-pooled siRNAs per gene target and each plate contained six non-targeting siRNA control wells. After 48 hr of transfection, cells were challenged with a *ΔsdhA* Lux^+ strain and luminescence was measured as a proxy for intracellular growth, performing the assay in at least triplicate samples for each gene target (Figure 1a). Candidates were identified by comparing the luminescence from each siRNA-treated well to the average luminescence of the non-targeting siRNA controls. The median absolute deviation score (ZMAD) was then determined for each gene target. We focused our analysis on early time points 12hpi and 24hpi because siRNA knockdown effects diminish after 72 hr of transfection, to identify candidates that stimulate *ΔsdhA* intracellular growth after depletion.

A total of 20 genes were identified as hits in the siRNA screen based on increased intracellular growth relative to the non-targeting siRNA controls with a cut-off of ZMAD ≥1.5. Candidate genes spanned functional roles in endocytosis, endocytic recycling and exocytosis (Figure 1c). Hits included arrestin subtypes (ARRB1 & ARRB2), clathrin heavy chain, regulators of actin cytoskeleton (ROCK1, CDC42, DNM2, ARFIP2, WASF1, VAV2), E3 ubiquitin ligase (NEDD4L), phosphoinositide kinase (PI3K), components of vesicle fusion (VAMP1 & SYT1) and specific Rab GTPase isoforms (RAB3D, RAB4B, RAB5B, RAB5C, RAB8A, RAB11B). Interestingly, only five

genes were identified as strong hits at both 12hpi and 24hpi (ARRB1, RAB3D, RAB4B, RAB5C, SYT1). Hits identified at 12hpi may alter pathways that are toxic for growth of bacteria during early steps of vacuole biogenesis, while hits identified at later times (such as DNM2 encoding a dynamin isoform) could block pathways that cause decay to an already established vacuole.

2.2 | Identification of shRNAs that partially rescue *ΔsdhA* vacuole integrity

The assay for increased bacterial yields allowed identification of knockdown candidates that could improve intracellular growth of the *ΔsdhA* mutant, but they may not increase the frequency of intact

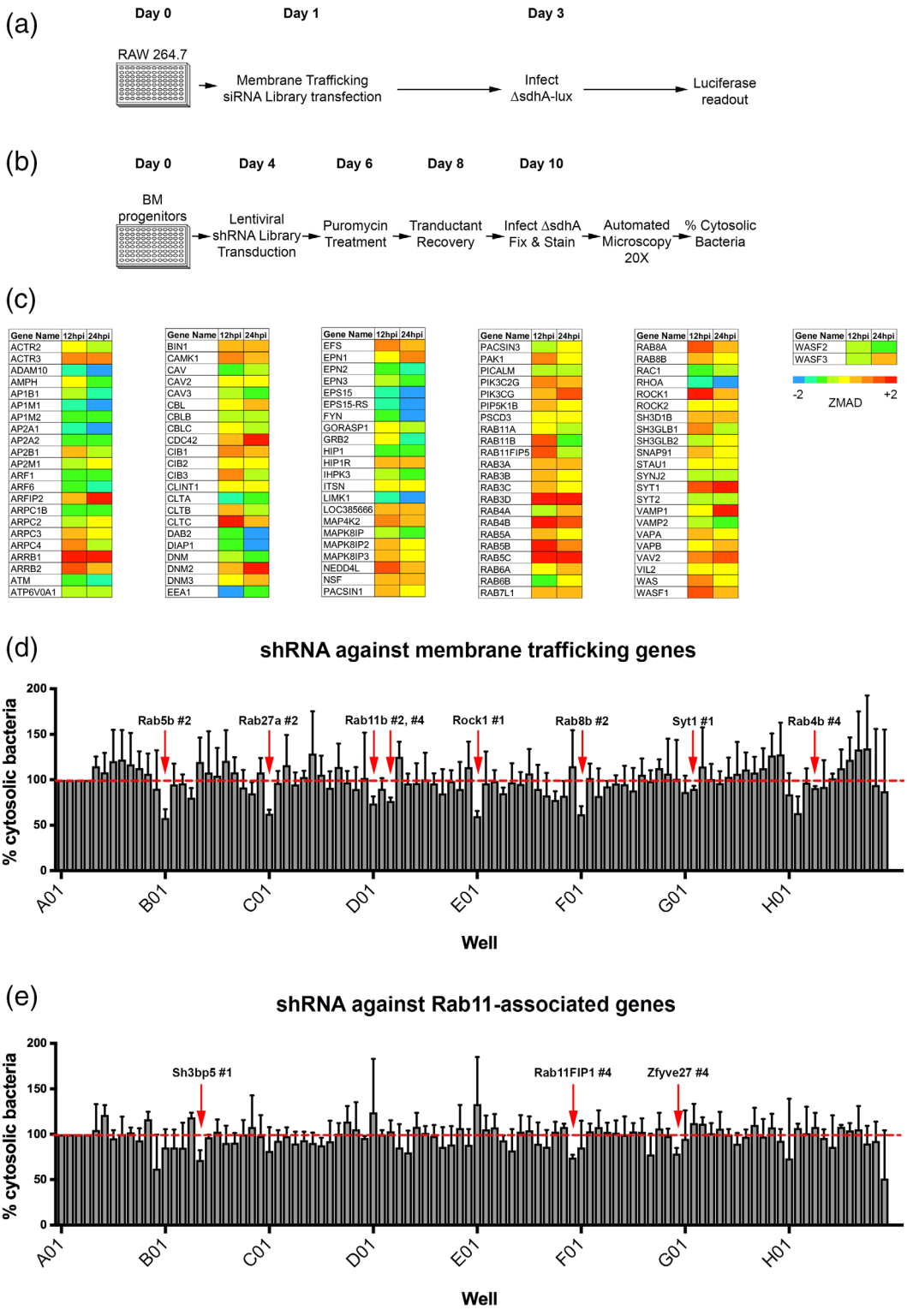

FIGURE 1 Legend on next page.

TABLE 1 Hits from shRNA lentiviral screens

Figure	Well	shRNA	Description/function	*p* value
2B	B01	Rab5b #2	Rab-GTPase. Endocytosis	.0172
2B	C01	Rab27a #2	Rab-GTPase. Exocytosis	.0048
2B	D01	Rab11b #2	Rab-GTPase. Endocytic vesicle recycling	.0293
2B	D03	Rab11b #4	Rab-GTPase. Endocytic vesicle recycling	.0091
2B	E01	Rock1 #1	Rho-associated protein kinase	.006
2B	F01	Rab8b #2	Rab-GTPase. Endocytic vesicle recycling	.0181
2B	G02	Syt1 #1	Synaptotagmin 1	.0346
2B	H04	Rab4b #4	Rab-GTPase. Endocytic vesicle recycling	.0172
2C	B05	Sh3bp5 #1	Rab11 GEF. Endocytic vesicle recycling	.044
2C	E12	Rab11FIP1 #4	Rab11 effector. Endocytic vesicle recycling	.0041
2C	F12	Zfyve27 #4	Protrudin. Endocytic vesicle recycling	.281

vacuoles. To directly test if improved growth was due to increased vacuole integrity, we selected hits from the siRNA screen and additional related targets for analysis in a secondary screen using a direct assay for vacuole integrity in bone marrow-derived macrophages (BMDM) from the mouse. The secondary screen took advantage of a fluorescence readout we previously described to detect disrupted *ΔsdhA* vacuoles in knockdown macrophages combined with shRNA knockdown in these primary cells (Creasey & Isberg, 2012). Terminally differentiated BMDMs were used to facilitate microscopic readout, and to avoid the complication of having a portion of the cells in S phase, which results in a high proportion of unstable vacuoles (de Jesus-Diaz, Murphy, Sol, Dorer, & Isberg, 2017). This strategy allowed subtle differences in vacuole integrity to be detected. BMDMs were transduced with a lentiviral shRNA library (Figure 1b) targeting 23 membrane trafficking genes arrayed as four individual shRNAs assayed separately (Table S2). Lentivirus encoding sh-LacZ was used as a control. After allowing differentiation and 6 days knockdown, BMDMs were challenged in triplicate with the *ΔsdhA* strain for 6 hr, fixed and probed for permeable vacuoles using the antibody accessibility assay (Creasey & Isberg, 2012). After capturing multiple images per well and subjecting them to image analysis to quantitate permeable vacuoles, shRNAs that increased the integrity of the *ΔsdhA* vacuole relative to the shRNA-LacZ negative control were identified (Figure 1d).

In this fashion, eight shRNAs were identified that significantly reduced the number of permeable *ΔsdhA* vacuoles detected in macrophages (Table 1, *t* test, $p = .0048–.0346$). The candidate genes included five members of the Rab family of GTPases that are associated with endocytic recycling, as well as ROCK1, and SYT1. Of this set, Rab5b, Rab11b and Rab8b were of particular interest due to their robust phenotype and their tight association with recycling, based on STRING analysis (Franceschini et al., 2013). Strikingly, two hits from the screen were shRNAs directed against Rab11b (Table 1), so this result was pursued further. Using the same screening procedures as described above, we performed a lentiviral shRNA library screen against gene targets related to Rab11 (Figure 1e). These gene targets included Rab11 guanine exchange factors (SH3BP5 & TRAPPC2L), motor proteins (MYO5B, KIF5A, KIF5B, KIF13A), adaptor protein (ZFYVE27), components of the exocyst complex (EXOC1-8), and downstream Rab11-family interacting proteins (RAB11FIP1–5) (Table S3). ShRNAs against SH3BP5, ZFYVE27 and RAB11FIP1 significantly reduced the number of disrupted *ΔsdhA* vacuoles detected in macrophages (Table 1; $p < .0041$ for RAB11FIP1). The gene target Rab11FIP1 was of particular interest, since this downstream Rab11 effector is known to

FIGURE 1 RNAi screens identify membrane trafficking proteins that antagonise *L. pneumophila ΔsdhA* intracellular growth and vacuole integrity. (a) Identification of siRNA that enhance intracellular growth. RAW 264.7 macrophages were seeded in 96-well plates and transfected the following day with a siRNA library directed against transcripts encoding membrane trafficking proteins. Transfected cells were challenged with *L. pneumophila ΔsdhA* Lux$^+$ and luminescence was measured at 12 and 24 hr post infection (hpi). (b) Identification of shRNAs that decrease vacuole permeability in primary macrophages. A/J bone marrow-derived progenitors were seeded in 96-well plates. Cells were transduced with shRNAs targeting genes identified in the siRNA screen (a). Terminally differentiated BMDM transductants were challenged with *ΔsdhA* for 6 hr. Plates were fixed and stained for cytosol-detected *L.p.* and total *L.p.*(c) Results of high-throughput siRNA screen for enhanced intracellular growth of *L. pneumophila ΔsdhA* Lux$^+$. Experimental design, Figure 1a, performing luminescence readings at 12 or 24 hpi, with least three replicate measurements for each gene target being performed Luminescence from each experimental well was normalised to the average luminescence of the non-targeting siRNA-treated control wells of the same plate. Normalised ZMAD values are shown colour-coded for each siRNA of the library. A cut-off of ZMAD ≥1.5 was used to select potential candidates. (d) Candidates identified in Figure 2a and additional targets not covered in the original screen were tested in a high-throughput shRNA screen, performing assay detailed in Figure 1b, detecting cytosolic exposure of bacteria. Three replicates for each knockdown condition were performed, capturing 16 images/well with automated microscopy. Image capture, analysis and normalisation of data were performed as described (Experimental Procedures). (e) Depletion of transcripts for a subset of Rab11 effectors results in increased vacuole integrity during *L. pneumophila ΔsdhA* intracellular growth. Assay conditions as in Figure 2b. Statistical analyses were performed on normalised data by unpaired *t* test (*$p < .05$) (Experimental Procedures)

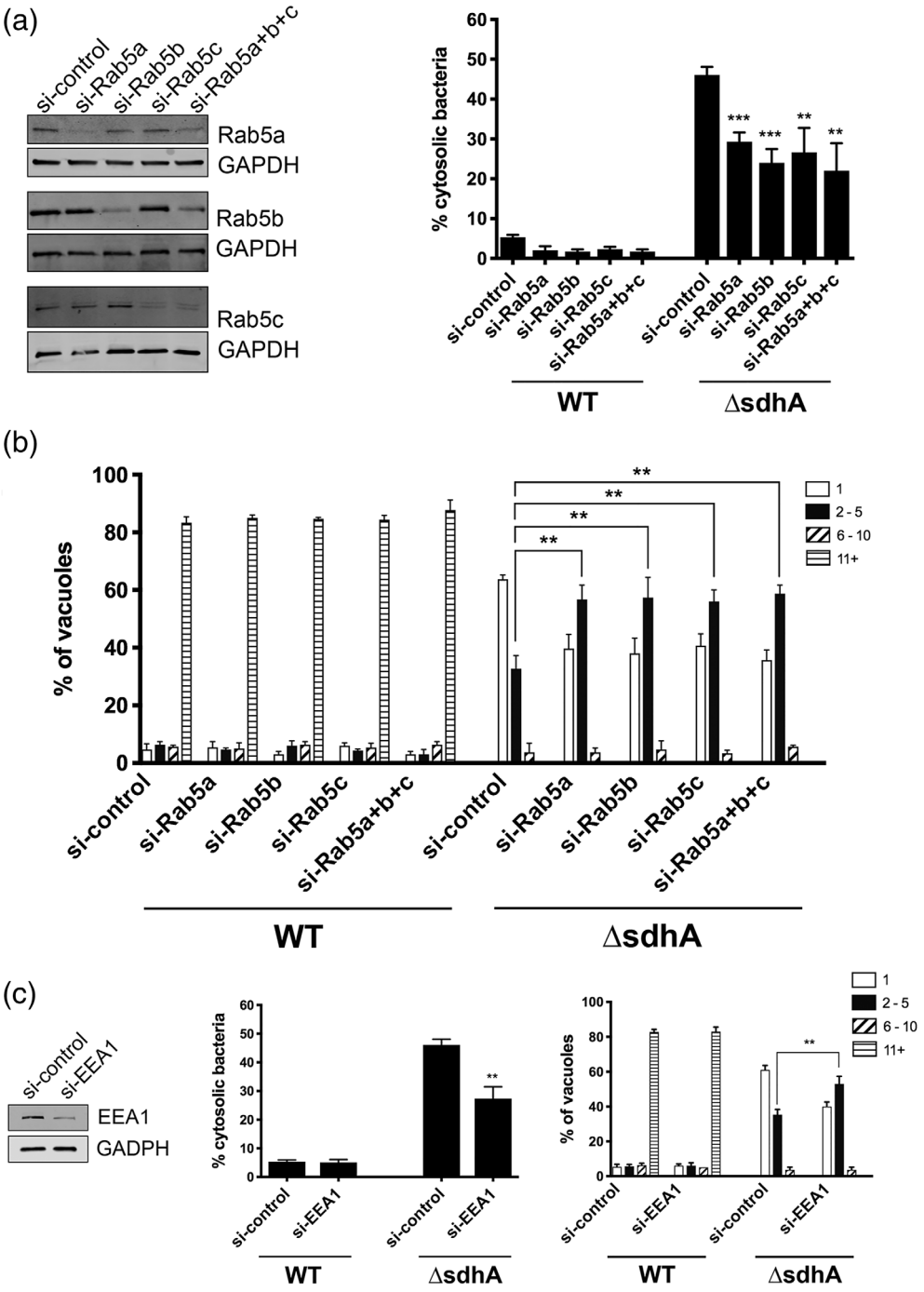

FIGURE 2 Depletion of proteins that control early endosome dynamics results in increased vacuole integrity after BMDM challenge with *L. pneumophila ΔsdhA*. (a) Depletion of Rab5 isoforms partially rescues *ΔsdhA* vacuole integrity. A/J bone marrow-derived macrophages were nucleofected with noted siRNAs. Knockdown efficiency was assessed by immunoblots with noted antibodies (left panels). Nucleofected macrophages were challenged with either WT or *ΔsdhA Legionella*, fixed at 6 hpi, and immunostained to determine cytosol exposure. Percent of cytosol-detected bacteria was quantified, as described (Experimental Procedures). (b) Growth of noted *L pneumophila* strains in nucleofected BMDM. After BMDMs were challenged for 14 hr, the cells were fixed and probed to determine yield of bacteria in each macrophage. Number of bacteria per vacuole were quantified microscopically, and binned into four groups, displaying the binned vacuole size based on the graph legend (Experimental Procedures; [Luo & Isberg, 2004]). (c) Depletion of downstream Rab5 effector EEA1 rescues *ΔsdhA* vacuole integrity and growth defects. Nucleofection, vacuole integrity and bacterial yields determined as in panels (a and b). Statistical analyses were performed on normalised data by unpaired *t* test (*<.05; **<.01; ***<.001; Experimental Procedures)

regulate membrane trafficking events and vesicle docking events (Horgan & McCaffrey, 2009; Welz, Wellbourne-Wood, & Kerkhoff, 2014). We selected Rab5b, Rab11b, Rab8b and Rab11FIP1 for further characterisation in response to a *ΔsdhA* infection.

2.3 | Interfering with early endosomal traffic stabilises the LCV harbouring the *ΔsdhA* mutant

Host membrane trafficking events are coordinated by small Rab GTPases in the cell (Pfeffer & Aivazian, 2004). Rab5 is involved in regulating endocytic trafficking events, and Rab11 and Rab8 regulate recycling events and anterograde transit (Stenmark, 2009). Little is known about how the *Legionella* vacuole subverts interaction with these Rabs and, specifically, their individual isoforms. A role for Rab5 isoforms in destabilising the LCV, in particular, was surprising because previous work with this protein favoured a model in which Rab5 acts to interfere with intracellular growth by driving the LCV into an endocytic or degradative compartment (Gaspar & Machner, 2014; Ku et al., 2012; Lucas et al., 2014). To determine if reduced Rab5 function can stabilise the vacuole harbouring the *ΔsdhA* strain, BMDMs were nucleofected with siRNAs against individual Rab isoforms and

knockdown efficiency was determined by immunoblot (Figure 2). Individual or group depletion of Rab5a, Rab5b, or Rab5c resulted in enhanced vacuole integrity in BMDM challenged with *L. pneumophila ΔsdhA* (Figure 2a). Furthermore, each individual knockdown resulted in enhanced intracellular growth of the *ΔsdhA* strain. In particular, initiation of intracellular replication was clearly revived in a subset of cells treated with the siRNA, although it was clear that growth restoration was far from complete (Figure 2b). This result was consistent with our previous experiments showing that increasing vacuole integrity in the absence of *SdhA* function only allows partial restoration of intracellular growth (Creasey & Isberg, 2012).

We next tested the effects on BMDMs that were treated with siRNA against EEA1, a Rab5 effector involved in promoting early endosome vesicle tethering, to determine if depletion of a well-

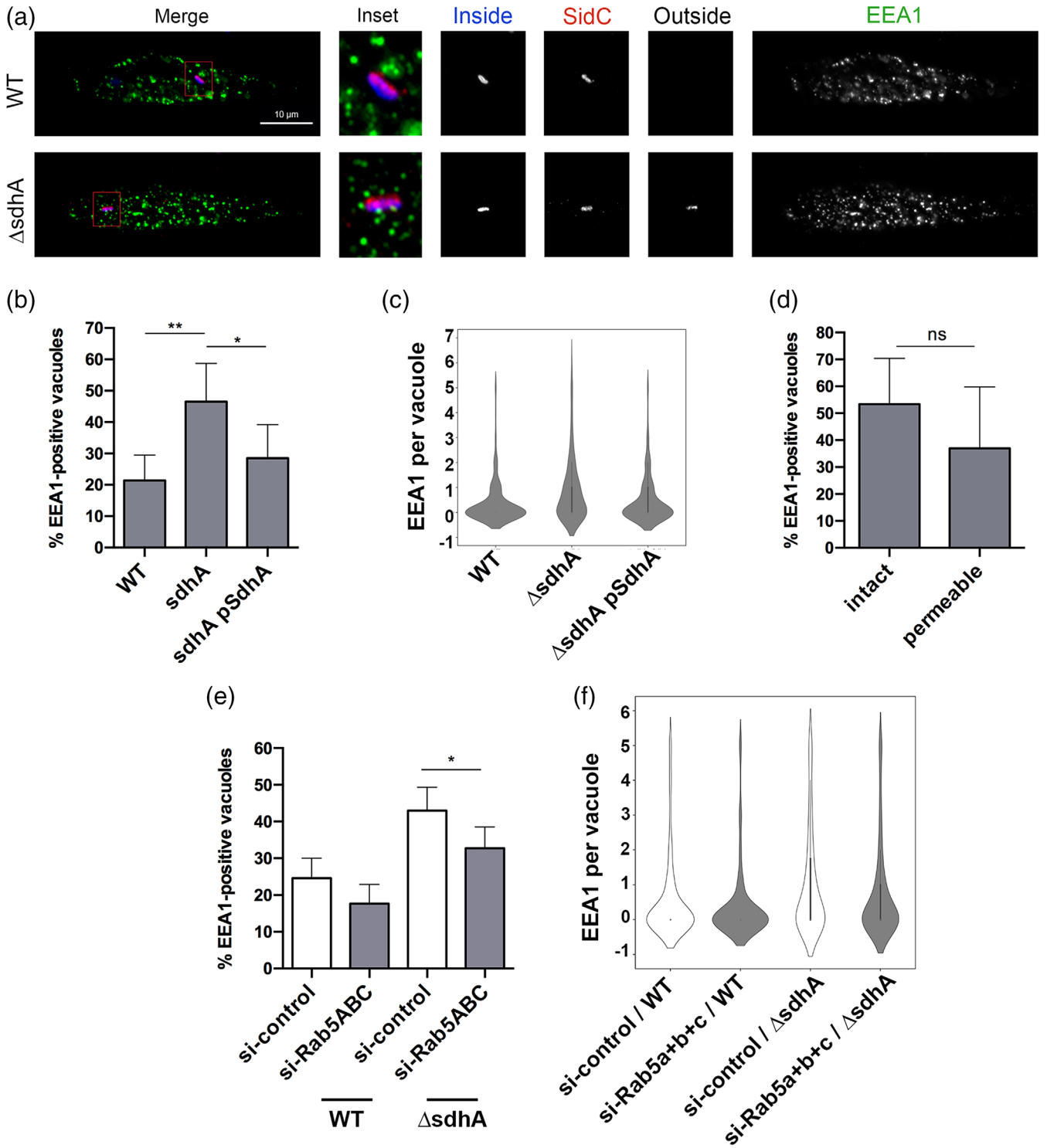

FIGURE 3 Legend on next page.

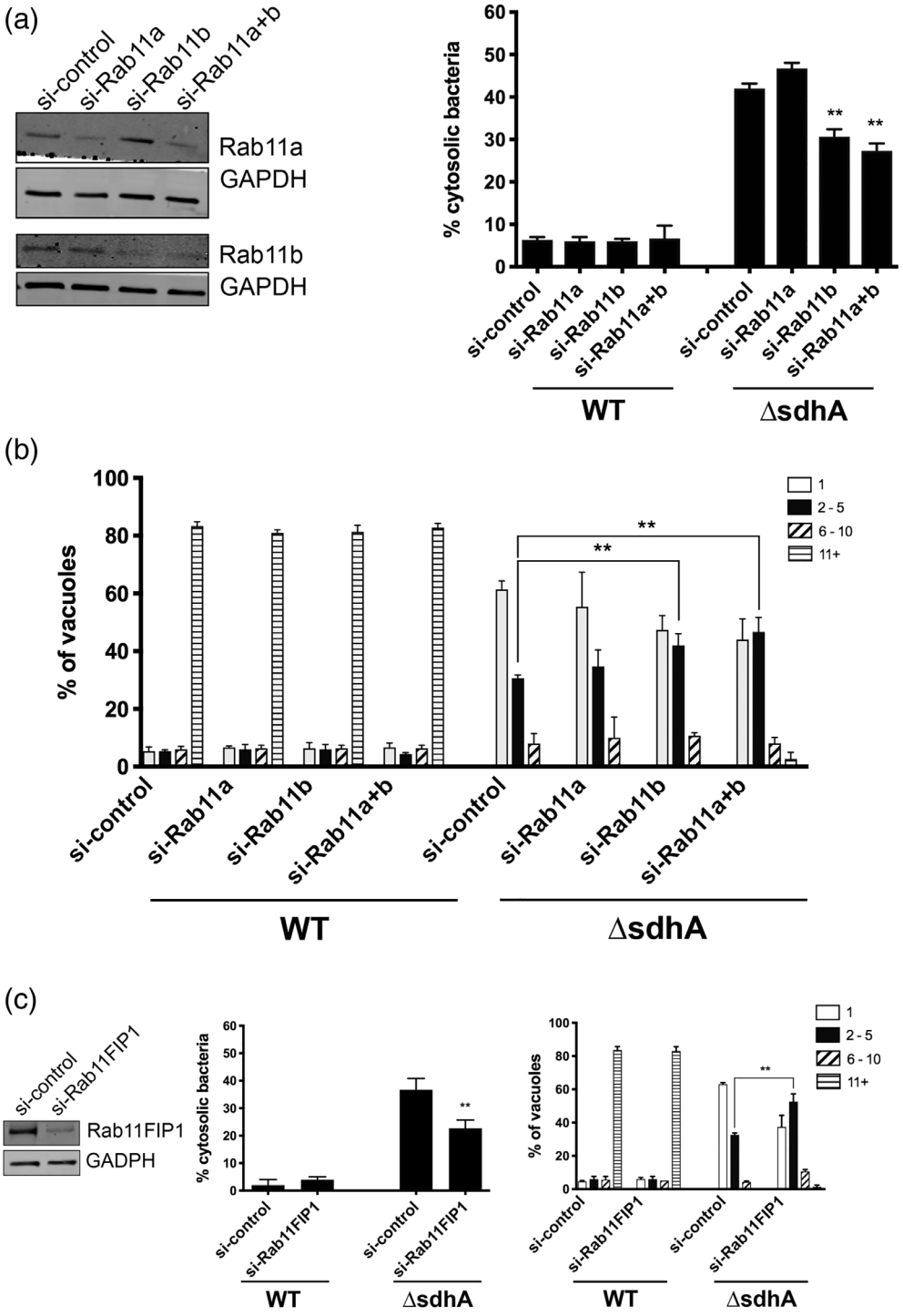

FIGURE 4 Depletion of proteins associated with recycling dynamics results in increased vacuole integrity after BMDM challenge with *L. pneumophila ΔsdhA*. (a) Specific depletion of Rab11b rescues *ΔsdhA* vacuole integrity. A/J bone marrow-derived macrophages were siRNAs treated as in Figure 2, and knockdown efficiency was assessed (left panels). Nucleofected macrophages were challenged with either WT or *ΔsdhA Legionella* and percent of cytosol-detected bacteria was quantified (Experimental Procedures). (b) Growth of noted *L pneumophila* strains in nucleofected BMDM for 14 hr. and quantified as described (Figure 2; Experimental Procedures; [Luo & Isberg, 2004]). (c) Depletion of Rab11 effector Fab11FIP1 rescues *ΔsdhA* vacuole integrity and growth defects. Nucleofection, vacuole integrity and bacterial yields determined as in panels (A and B). Statistical analyses were performed on normalised data by unpaired *t* test (*<.05; **<.01; ***<.001; Experimental Procedures)

FIGURE 3 The *SdhA* protein interferes with contact of early endosomal compartments with the LCV. (a) Representative immunofluorescence microscopy images of the *Legionella*-containing vacuole in infected BMDMs at 4hpi, challenged with noted bacterial strains. Cells were probed with anti-*L. pneumophila* before and after permeabilisation, to determine vacuole integrity (Experimental Procedures) as well as anti-SidC and anti-EEA1 after permeabilisation. EEA1 and SidC are pseudo-coloured in green and red, respectively. Insets are magnified 3.25-fold from the original image by changing resolution. Other panels are identical resolution to original grabbed images. (b) Images from (a) were analysed to quantify EEA1 events (Experimental Procedures). Total of 146 vacuoles from two experiments were analysed. (c) Frequency distribution of events from (b). Interquartile range was calculated from integer values. (d) Lack of correlation between intact or cytosol-detected (permeable) *ΔsdhA* vacuoles and distribution of EEA1-containing compartments at the vacuole. (e) BMDMs nucleofected with siRNA were challenged with noted *L. pneumophila* strains and stained as in (a). Images were captured and analysed after capture to determine localisation of EEA1 near the vacuole) (Experimental Procedures). Total of 182 vacuoles from two experiments were analysed. (f) Frequency distribution of localisation events from (e). Interquartile range was calculated from integer values. Statistical tests were as in Figure 2

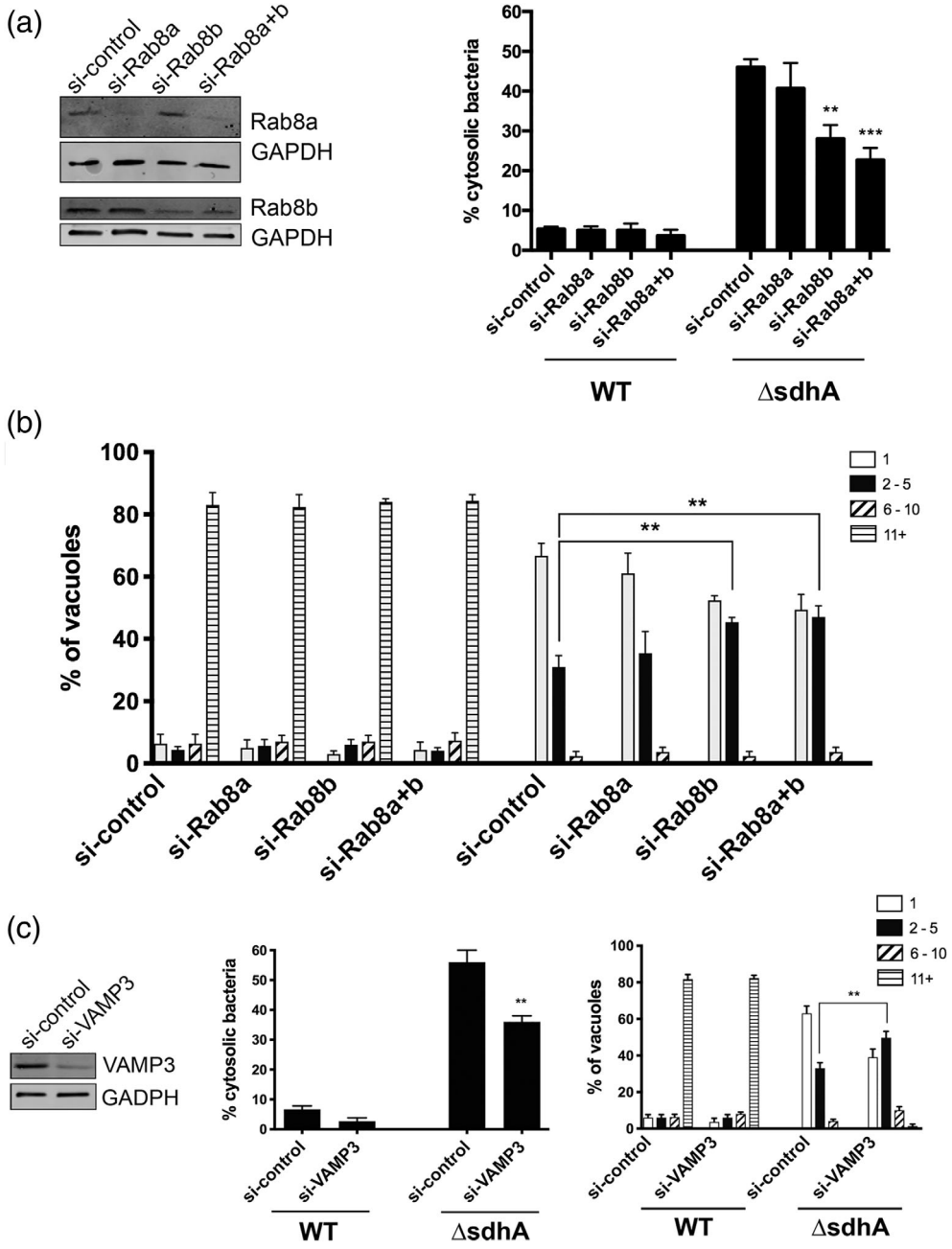

FIGURE 5 Depletion of anterograde transport Rab8b and a downstream effector reduces bacterial cytosolic exposure. (a) Depletion of Rab8b rescues *ΔsdhA* vacuole integrity. A/J bone marrow-derived macrophages were siRNAs treated and knockdown efficiency was assessed (left panels). Nucleofected macrophages were challenged with either WT or *ΔsdhA Legionella* and percent of cytosol-detected bacteria was quantified (Experimental Procedures). (b) Growth of noted *L pneumophila* strains in nucleofected BMDM for 14 hr and quantified as described (Figure 2; Experimental Procedures; [Luo & Isberg, 2004]). (c) Depletion of Rab8 and Rab11 effector VAMP3 rescues *ΔsdhA* vacuole integrity and growth defects. Nucleofection, vacuole integrity and bacterial yields determined as in panels (A and B). Statistical analyses were performed on normalised data by unpaired *t* test (*<.05; **<.01; ***<.001; Experimental Procedures)

characterised target of Rab5 could have similar effects (Christoforidis, McBride, Burgoyne, & Zerial, 1999). Depletion of EEA1 in BMDM with an siRNA pool showed lowered steady-state levels of the protein that were accompanied by a decrease in the number of cytosol-exposed *L. pneumophila ΔsdhA* after 6 hr. infection (Figure 2c). Depletion of EEA1 had effects on intracellular growth of the *ΔsdhA* strain that were similar to those observed with Rab5 isoform depletions (Figure 2b). These results are consistent with early endosome traffic playing a role in destabilising the LCV harbouring the *ΔsdhA* strain, perhaps because early endosomes are trafficked proximally to the *ΔsdhA* vacuole, resulting in vacuole disruption in the absence of *SdhA* function.

A model for the action of the *SdhA* protein is that it acts to limit access of material from early endosomes to the LCV. As EEA1 depletion reduced vacuole permeabilisation, and this protein is an important component of early endosomes, the localisation of EEA1-positive compartments around LCVs was determined after challenge of macrophages (Figure 3). After 4 hr of challenge, BMDMs were fixed and simultaneously stained for EEA1, cytosol-accessible bacteria, total bacteria, and SidC, a marker of the LCV membrane (Luo & Isberg, 2004; Weber, Ragaz, Reus, Nyfeler, & Hilbi, 2006). EEA1-positive puncta were dispersed throughout the cell, and localisation of the puncta around the LCV was determined by image analysis, quantifying the density of EEA1-associated compartments around the vacuole (Figure 3a; Experimental Procedures). The density of EEA1 increased significantly nearby the *ΔsdhA* vacuole compared to the WT vacuole (Figure 3a,b), consistent with EEA1 function

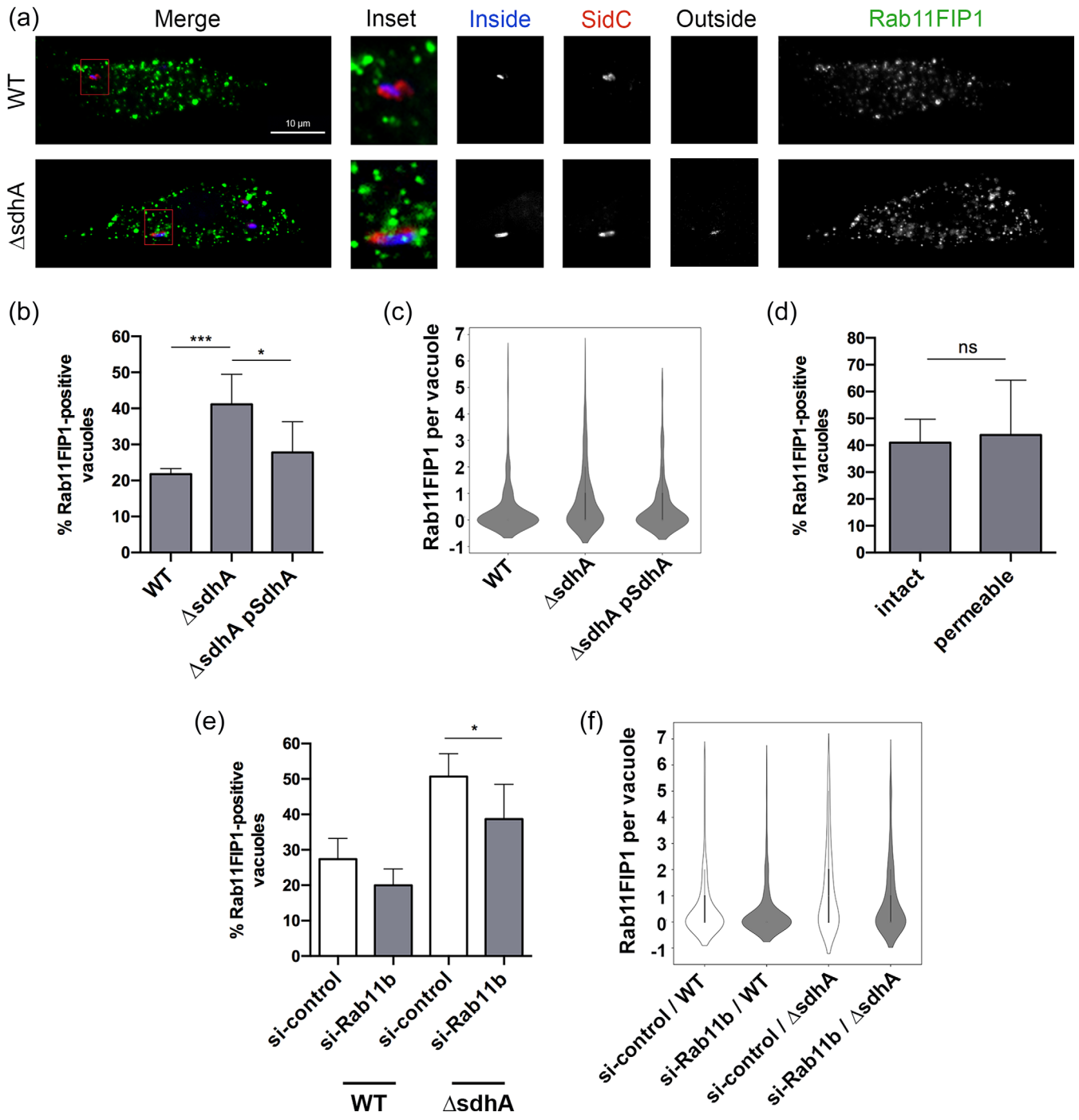

FIGURE 6 *SdhA* functions to interfere with Rab11FIP1-LCV interactions. (a) Representative immunofluorescence microscopy images of the *Legionella*-containing vacuole in infected BMDMs at 4hpi, challenged with noted bacterial strains. Cells were probed with anti-*L. pneumophila* before and after permeabilisation, to determine vacuole integrity (Experimental Procedures) as well as anti-Rab11FIP1 and SidC after permeabilisation. Rab11FIP1 and SidC are pseudo-coloured in green and red, respectively. Insets are magnified 3.25-fold from the original image by changing resolution. Other panels are identical resolution to original grabbed images. (b) Images from (a) were analysed in Volocity to quantify localisation events of Rab11FIP1. Total of 181 vacuoles from two experiments were analysed. (c) Frequency distribution of localisation events from (b). Interquartile range was calculated from integer values. (d) Lack of correlation between intact or cytosol-detected (permeable) *ΔsdhA* vacuoles and density of Rab11FIP1 near the vacuole. (e) BMDMs were nucleofected with siRNA, were challenged with noted *L. pneumophila* strains and stained as in (a). Images were captured and analysed after capture to quantify density of Rab11FIP-associated compartments at the vacuole (Experimental Procedures). Total of 158 vacuoles from two experiments were analysed. (f) Frequency distribution of events from (e). Interquartile range was calculated from integer values

playing a role in vacuole destabilisation (Figure 2c). Furthermore, this phenotype was rescued by introduction of a plasmid encoding *SdhA* in the *L. pneumophila ΔsdhA* mutant (Figure 3b,c). There was no significant correlation between intact or disrupted *ΔsdhA* vacuoles and the EEA1 redistribution, which may be a reflection of transient interactions that cannot be captured by fixed cell assays (Figure 3d).

If aberrant increased localisation of EEA1 with the *ΔsdhA* LCV is due to the action of Rab5, then knockdown of Rab isoforms should reverse this effect. As expected, simultaneous knockdown of all three Rab5 isoforms in BMDMS reduced the number of EEA1-positive compartments associated with Δ*sdhA* LCV during infection (Figure 3e,f). Therefore, Rab5 isoforms play a role in loss of LCV integrity, causing increased association of EEA1 with the dysfunctional *Legionella ΔsdhA*-containing compartment. This result is consistent with proposition that the compartments decorated by EEA1 contribute to this loss of integrity and a function of *SdhA* protein is to interfere with this traffic.

2.3.1 | A role for membrane egress pathways in destabilising the *ΔsdhA* mutant

In contrast to Rab5, regulators of anterograde or recycling traffic such as Rab8 and Rab11 have not been associated with restriction of *L. pneumophila* intracellular growth. On the other hand, Rab11a has been connected to regulated disintegration of the *Shigella* vacuole (Mellouk et al., 2014; Weiner et al., 2016). The identification of knockdown candidates that were downstream effectors of Rab11 (Rab11Fip1; Figure 1d) and Rab8 (Vamp3; Figure 5) supports a role for these proteins in destabilising the LCV surrounding the *ΔsdhA* mutant (Banerjee et al., 2017; Christoforidis et al., 1999; Finetti et al., 2015; Lindsay & McCaffrey, 2004; Wilcke et al., 2000). Surprisingly, only depletion of the Rab11b isoform of Rab11 decreased bacterial exposure to the cytosol after challenge of BMDM with the *ΔsdhA* mutant (Figure 4a). Depletion of Rab11a did not rescue the *ΔsdhA* phenotypic defects, while double knockdowns of Rab11a and Rab11b mimicked the defects exhibited by the single depletions that showed rescue (Figure 4a). Similarly, only siRNA treatment directed against Rab11b resulted in an increase in the bacterial yield of the *ΔsdhA* mutant within LCVs, arguing that the effects are highly isoform-specific (Figure 4b). Similar to the results with Rab5 and other strategies that increase the integrity of the *ΔsdhA* mutant-containing LCV, the stimulation of growth was relatively limited (Creasey & Isberg, 2012).

From the secondary shRNA screen in BMDMs, we found that silencing Rab11 downstream effector Rab11FIP1 restored *ΔsdhA* vacuole integrity (Figure 1e). Nucleofection of BMDMs with siRNA targeting a different region of Rab11FIP1 provided the identical result and demonstrated that depletion of this protein rescued Δ*sdhA* vacuole integrity and growth (Figure 4c). Given that several downstream effectors of Rab11 that were targeted by our secondary siRNA screen showed no clear enhancement of LCV integrity (Figure 1e), this argues that a specific membrane trafficking pathway promoted by the Rab11B isoform and acting through Rab11FIP1 destabilises the LCV surrounding the *ΔsdhA* mutant. Depletion of Rab11b in combination with either Rab11FIP1 or Rab5b did not result in further decrease of cytosolic exposure of bacteria, indicating that all may work via the same pathway (Figure S1).

Paralleling our results with Rab11, only depletion of the Rab8b isoform showed significant reduction in permeability of the *ΔsdhA* LCV (Figure 5a), resulting in increased intracellular growth (Figure 5b). When measuring LCV permeability, however, dual depletion with Rab8a and Rab8b increased the statistical significance of this result (Figure 5a), indicating that the two proteins may have partial overlap in function. Of particular note regarding the vacuole integrity readouts, both shRNA (Figure 1d) and siRNA in primary macrophages (Figures 4 and 5) gave identical results for both the Rab8 and Rab11 isoforms, further supporting isoform specificity. Similar to knockdown of Rab5 and Rab8 effectors, siRNA directed against VAMP3, a SNARE protein that promotes vesicle fusion events and is a downstream effector of both Rab11 and Rab8, was sufficient to partially restore *ΔsdhA* vacuole integrity and intracellular growth (Banerjee et al., 2017; Christoforidis et al., 1999; Finetti et al., 2015; Lindsay & McCaffrey, 2004; Wilcke et al., 2000) (Figure 5c).

Based on these findings, we expect that membrane material driven by these GTPases will be closely associated with the *ΔsdhA* LCV, contributing to vacuole disruption. In the presence of *SdhA* function, in contrast, access to these compartments should be limited. To this end, the localisation of the Rab11 effector FIP1 was analysed, using the same assay employed to detect EEA1 localisation (Figure 3). BMDM challenged for 4 hr with either WT or *ΔsdhA* strain was fixed and probed for vacuole permeability, and the association of Rab11FIP1 with the LCV was determined (Figure 6). Antibody against Rab11FIP1 labelled distinct puncta dispersed throughout the cell (Figure 6a). Similar to EEA1, there was a higher density of Rab11FIP1 about the *ΔsdhA* vacuole compared to the WT vacuole, with the phenotype rescued by complementation of SdhA on plasmid *in trans* (Figure 6b,c). Again, we observed no significant correlation between intact or disrupted *ΔsdhA* vacuoles and Rab11FIP1 density distribution (Figure 6d). Similar to the results obtained with Rab5 and EEA1 localisation, knockdown of the Rab11b isoform reduced the number of Rab11FIP1 compartments associated with the Δ*sdhA* vacuole (Figure 6e, f). This argues that in the absence of *SdhA* function, the heightened level of Rab11FIP1-staining material associated with the LCV is a consequence of Rab11b trafficking events that result in vacuole disruption.

3 | DISCUSSION

In this study, screens were performed that identified host membrane trafficking factors responsible for causing vacuole disruption and interfering with intracellular growth of an *L. pneumophila ΔsdhA* strain. We initially used a luciferase reporter assay to positively select for siRNA-depleted cells that showed increased intracellular growth of the mutant strain. Overall, 20 candidate genes were identified after screening 112 genes. To demonstrate specificity for knockdowns that result in increased LCV integrity relative to that observed in BMDMs, we turned to high-throughput microscopy analysis to identify factors specifically involved in antagonising vacuole integrity of the *L. pneumophila ΔsdhA*

mutant. From a primary shRNA screen introduced into BMDMs by lentivirus, we identified eight candidate genes, with the majority being Rab GTPases involved in endocytic and membrane recycling. Genes of particular interest were Rab5, Rab8 and Rab11. Strikingly, Rab11a had been previously shown to regulate vacuole rupture as an early event that supports intracellular growth of *Shigella* after uptake into cultured cells (Mellouk et al., 2014; Weiner et al., 2016). This raises the possibility that trafficking events that support intracellular growth of a cytosolic pathogen (*S. flexneri*) interfere with the biogenesis of the membrane surrounding an intravacuolar organism (*L. pneumophila*).

Validation of screen hits revealed that rescue of *ΔsdhA* vacuole integrity and growth was specific to depletion of individual isoforms. One exception to this observation was silencing Rab5a, Rab5b or Rab5c, in which we found that individual depletion of each isoform was sufficient to reduce vacuole disruption (Figure 2a). This phenotype is consistent with previous studies demonstrating that the three isoforms localise to the same endocytic compartment and cooperatively regulate endocytic events (Bucci et al., 1995). Depletion of all three isoforms rescued the *ΔsdhA* phenotype to a similar degree as the depletion of individual isoforms, indicating that the isoforms function collectively rather than separately during trafficking.

In contrast to the situation with the Rab5 isoforms, specific silencing of Rab11b, but not Rab11a, enhanced the integrity of the *ΔsdhA* vacuole (Figure 4a). Furthermore, knockdown of both Rab11 isoforms produced a similar phenotype as individual knockdown of Rab11b, confirming that only Rab11b is required for *ΔsdhA* vacuole disruption. It has been shown in other cell types that these two isoforms can localise to distinct compartments within the cell, consistent with a division of function between the two isoforms that is linked to their association with different compartments (Kelly, Horgan, & McCaffrey, 2012; Lapierre et al., 2003). Of particular note in this regard is that the Rab11a isoform specifically supports growth of *S. flexneri*. The isoform differences between the two pathogens may reflect spatial and temporal differences in the biogenesis and degradation of the bacterium-containing compartments. After uptake into host cells, depletion of Rab11a interferes with degradation of the *Shigella*-containing vacuole, while Rab11b has no documented effect. As degradation of the *Shigella*-containing vacuole occurs shortly after bacterial uptake at the periphery of cells, Rab11a may drive compartment destabilisation in this region. In contrast, *Legionella* vacuole degradation occurs hours after infection, allowing access to perinuclear regions that could allow an interface with Rab11b-containing compartments.

A similar phenomenon was discovered when individual Rab8 isoforms were depleted in primary macrophages. Silencing of Rab8b, but not Rab8a, increased the stability of vacuoles harbouring the *ΔsdhA* strain and resulted in enhanced growth for the mutant (Figure 5a). Very little is known about the difference between the two Rab8 isoforms, although it is postulated that they function in both distinct and overlapping compartments in various cell types (Chen, Liang, Chia, Ngsee, & Ting, 2001; Sato et al., 2014). Unlike the situation with Rab11a/b, experimental knockdown of Rab8a in combination with Rab8b enhances rescue relative to individual depletion of the Rab8b isoform. This additive effect is consistent with a small pool of Rab8a that has either overlapping function or overlapping localisation with Rab8b, resulting in a fraction of the *ΔsdhA*-containing vacuoles being destabilised by the Rab8a isoform.

We investigated if downstream effectors of the Rab GTPases were involved in facilitating *ΔsdhA* vacuole disruption. We demonstrated that depletion of the Rab5 effector EEA1 and the Rab11b effector Rab11FIP1 partially restored integrity of the *ΔsdhA*-containing vacuole and increased intracellular growth of the mutant, generating phenotypes indistinguishable from depletion of the GTPases (Figures 2c and 4c). We also found that depletion of VAMP3, a downstream regulator fusion event controlled by both Rab8b and Rab11b, could result in an increased number of intact vacuoles harbouring the *ΔsdhA* strain (Figure 5c) (Banerjee et al., 2017; Finetti et al., 2015; Wilcke et al., 2000). VAMP3 is SNARE protein that drives membrane fusion, thus pointing to a model in which disruption of membrane integrity is a consequence of fusion with a compartment that destabilises the LCV (Hu, Hardee, & Minnear, 2007).

The effectors implicated in vacuole destabilisation are consistent with their defining either two different types of compartments that can destabilise the LCV or identifying distinct steps in the destabilisation process. We found that depletion of Rab5 isoforms or Rab11b decreased the percentage of EEA1 and Rab11FIP1 localisation near the *ΔsdhA* vacuole, respectively. EEA1 is involved in *tethering* Rab5-positive endosomes to membranes enriched in PI(3)P while Rab11FIP1 is known to be involved in *docking* recycling vesicles to membranes enriched in PI(3,4,5,)P_3 (Christoforidis et al., 1999; Lindsay & McCaffrey, 2004). Therefore, the nature of the lipid components could define different compartments, or these proteins could define tethering (EEA1), docking (Rab11Fip1) and fusion (Vamp3) events. Consistent with either model, we found that EEA1 and Rab11FIP1 localised to the *ΔsdhA*-containing vacuole with was a higher density compared to the WT-containing vacuole, indicating that they may play a direct role in destabilising the vacuole harbouring the mutant (Figures 3 and 6). One of the striking properties of the LCV is that it appears to be walled off from the host early endosomal trafficking system (Isberg et al., 2009). The presence of EEA1 associated with events leading to vacuole rupture indicates that constructing of such a firewall is essential for preserving vacuole integrity.

The mechanical details of *ΔsdhA* vacuole disruption remain unclear. Surprisingly, neither EEA1 nor Rab11FIP1 recruitment showed any preference for intact or disrupted vacuoles harbouring the *ΔsdhA* strain. Vacuole interactions with destabilising compartments could be transient, making it difficult to distinguish differences based on single time point assays. If an efficient transfection system in macrophages can be developed that allows real-time analysis of membrane trafficking in relevant cells, then transient interactions may be identified in real time that were lost in the snapshot-type experiments described in our study. A second complication is that if a variety of membrane compartments can destabilise the LCV, probing for only two proteins will not capture the total spectrum of disruptive compartments. Of note is the possibility that the increased frequency of EEA1 and Rab11FIP1 at the *ΔsdhA* vacuole compared to WT identifies a phospholipid motif that signals for self-destruction of the

compartment by a number of membrane trafficking events. Consistent with the formation of a unique lipid environment in response to the *sdhA* mutant, the compartment is particularly sensitive to the action of the *L. pneumophila* lysophospholipase PlaA (Creasey & Isberg, 2012). Presumably, lipids are found on this vacuole, which are missing from the WT, in turn serving as substrates for PlaA.

It appears likely that the destabilisation events and unique lipid environment leading to destabilisation result from the combined action of vesicular traffic and bacterial proteins. The basis for this hypothesis is that there is little evidence that tethering and/or docking of endocytic compartments can lead to membrane destruction, without microbial intervention so presumably an effector makes the compartment particularly sensitive to manipulation by endocytic or recycling compartments. It is possible that the membrane disruption events modulated by Rabs normally take place prior to spread into other hosts, as termination of the replication cycle involves lysis of the vacuole and disintegration of the host cell plasma membrane. *SdhA* may prevent these events from occurring prematurely. By this formation, bacterial effectors are placed in the LCV membrane that allows targeting of specific Rab isoforms, such as Rab11a. *SdhA* prevents these targeting events from occurring until the LCV becomes engorged, at which time, vacuole disruption events normally blocked by *SdhA* drive an important step in terminating the replication cycle within the cell.

Not considered here is the possibility that cargo being delivered to the *ΔsdhA* vacuole from the endocytic-recycling pathway directly destroys membranes. Delivery of toxic cargo to the bacteria-containing vacuole has been observed in other pathogens, such as *Salmonella* (McGourty et al., 2012). It has been demonstrated in macrophages that Rab11 traffics the NADPH oxidase flavocytochrome B, and it is possible that this cargo could be delivered to the *ΔsdhA* vacuole resulting in oxidative destabilisation (Casbon, Allen, Dunn, & Dinauer, 2009). It is interesting to note that vacuole degradation is an essential step necessary to release *S. flexneri* into the cytosol and initiate intracellular replication. These events appear to require recruitment of Rab11A-containing vesicles that could carry destabilising cargo (Mellouk et al., 2014; Weiner et al., 2016). Therefore, an event that for one pathogen is toxic, for another is an essential step in the biogenesis process leading to intracellular growth.

Altogether, this study describes a genetic screen that identified a specific set of host factors that are required for *ΔsdhA* vacuole disruption. Future studies should elucidate the exact mechanism by which these proteins facilitate vacuole disruption and the nature of the cargo being delivered to the vacuole that destabilises the vacuole.

4 | EXPERIMENTAL PROCEDURES

4.1 | Bacterial culture and media

All *L. pneumophila* strains used in this study are derived from the Philadelphia 1 isolate and are described in Table 2 (Berger & Isberg, 1993). Luminescent *L. pneumophila* was constructed using P_{ahpC}::*luxCDABE* as previously described (Coers, Vance, Fontana, & Dietrich, 2007; Ensminger, Yassin, Miron, & Isberg, 2012). *L. pneumophila* strains were grown on plates containing charcoal and yeast extract buffered with ACES [N-(2-acetamido)-2-aminoethanesulfonic; Sigma] adjusted to pH 6.9 and supplemented with 0.4 mg/ml of L-cysteine and 0.135 mg/ml of ferric nitrate (CYE), as well as 0.1 mg/ml thymidine and/or kanamycin (Sigma) when necessary. Liquid cultures of *L. pneumophila* were prepared in the same medium, but without charcoal and agar (AYE) (de Jesus-Diaz et al., 2017). Overnight *L. pneumophila* cultures were prepared by inoculating AYE broth with a bacterial patch and serially diluting cultures 1–2. Liquid cultures were incubated overnight at 37°C with shaking. For infections, overnight cultures were used, and all strains were grown to post-exponential phase (A_{600} of 3.5–4.0) (Byrne & Swanson, 1998). The approximate multiplicities of infection were determined by assuming that an A_{600} = 1.0 is equivalent to 10^9 bacteria/ml.

4.2 | Mammalian cell culture

RAW 264.7 cells (ATCC TIB-71) were grown in Dulbecco's modified Eagle medium (DMEM, Gibco) supplemented with heat-inactivated fetal bovine serum (FBS). BMDMs were isolated from femurs and tibias of female A/J mice as previously described and frozen in heat-inactivated FBS with 10% dimethyl sulfoxide (Auerbuch, Golenbock, & Isberg, 2009). BMDMs were plated in RPMI 1640 (Gibco) rab5-emented with 10% heat-inactivated FBS (Invitrogen) and 1 mM L-glutamine (Gibco) 1 day prior to challenge with *L. pneumophila*. Animal protocols were approved by the Institutional Animal Care and Use Committee of Tufts University.

4.3 | Primary siRNA library screen

The Mouse siGENOME siRNA Library of 112 siRNA directed against membrane trafficking genes (Dharmacon, Lafayette, CO; GU-015500) was tested in a high-throughput screen. The library consists of a pool of four different oligos for each target gene. RAW 264.7 cells were seeded overnight in RPMI medium (Thermo Fisher Scientific)

TABLE 2 Strains used in this study

Strain/ plasmid	Genotype	Description	Reference
WT	Lp02, Philadelphia-1, rpsL hsdR thyA–	Wild-type strain	Berger and Isberg, (1993)
Δ*sdhA*	Lp02 Δ*sdhA*	*SdhA* deletion	Creasey and Isberg, (2012)
Δ*sdhA* lux+	Lp02 Δ*sdhA* kan^R P_{ahpC}::Lux	*SdhA* deletion, lux+	This study
p*SdhA*	pJB908*sdhA*	Expression vector for *SdhA*	Creasey and Isberg, 2012

containing 10% (vol/vol) FBS at a density of 1.25×10^4 cells per well in a 96-well white-bottom plate (Thermo Fisher Scientific). The next day, the cells were transfected with 50 nM siRNA using Lipofectamine RNAiMAX Reagent (Thermo Fisher Scientific). The screen was designed with three negative control wells, transfected with non-targeting siRNA, and one well for each experimental siRNA target. After 24 hr of transfection, the medium was replaced to reduce cell cytotoxicity. After 48 hr of transfection, cells were challenged at an MOI = 0.5 with *L. pneumophila ΔsdhA* Lux $^+$ grown to post-exponential phase. At 1 hr post-challenge, extracellular bacteria were removed by washing in PBS and cells were incubated at 37°C, 5% CO_2 in Phenol Red-free RPMI media containing 10% FBS. Relative light units (RLU) of each well were measured every 12 hr in a Tecan M200 Pro plate reader. A total of eight plates were screened to collect at least three replicate measurements for each gene target. RLU from each experimental well was normalised to the average RLU of the negative control wells on the same plate. Using normalised data, Z_{MAD} scores (equivalent the number of median absolute deviations [MAD] from the median) were calculated for each experimental siRNA target and were used for selection of hits (Chung et al., 2008). The classification of the scale of the siRNA effects based on the ZMAD score was defined as follow: |ZMAD| ≥ 2 for extremely strong RLU, 2 > |ZMAD| ≥ 1.5 for very strong RLU, 1.5 > |ZMAD| ≥ 1 for strong RLU, 1 > |ZMAD| ≥ 0.5 for moderately strong RLU, 0.5 > |ZMAD| ≥ 0 for no effect, 0 > |ZMAD| ≥ −0.5 for moderately weak RLU, −0.5 > |ZMAD| ≥ −1 for weak RLU, −1 > |ZMAD| ≥ −1.5 for very weak RLU, −1.5 > |ZMAD| for extremely weak RLU. Only siRNAs that had a ZMAD of ≥1.5 were considered of interest for further analysis in the secondary shRNA library screen, as described next.

4.4 | Secondary shRNA library screen

Selected hits from the primary siRNA library screen and additional related targets were tested in a screen using shRNA constructions introduced into BMDMs. The shRNA were obtained from the Broad Institute Genetic Pertubation Platform (https://www.broadinstitute.org/genetic-perturbation-platform). To this end, lentiviral vector library plates were constructed with three negative control shRNAs against LacZ and 92 experimental lentiviral shRNAs against 23 target genes (four shRNAs per target). All shRNAs were contained on third-generation transfer plasmid pLKO.1, which confers puromycin resistance. On day 0, progenitor cells derived from the bone marrow of A/J mice (Experimental Procedures) were seeded at a density of 5×10^4 cells per well in a 96-well clear-bottom black plate (Corning) in RPMI medium containing 30% (vol/vol) L-cell supernatant, 20% FBS and 1% penicillin–streptomycin (BMM media, Gibco). On day 4, polybrene (Sigma) and 2×10^5 infectious units of lentivirus were added to the wells, and transduction was initiated by centrifugation at 2,200 rpm at 37°C for 20 min. On day 5, conditioned medium was replaced to reduce cell cytotoxicity. On day 6, transductants were selected in conditioned medium containing 3 μg/ml puromycin. On day 8, the supernatants were removed and replaced with puromycin-free conditioned medium to recover transduced clones. On day 10, the cultured medium was changed to RPMI containing 10% FBS. Terminally differentiated macrophage transductants were challenged with *L. pneumophila ΔsdhA* at MOI = 1 for 1 hr, followed by removal of extracellular bacteria by washing in PBS. After 6 hr, infected macrophages were fixed with 4% (vol/vol) paraformaldehyde in PBS and disrupted vacuoles were stained as described in "Vacuole Integrity & Intracellular Replication Assay." The screen was performed on triplicate shRNA library and plates were stored in PBS at 4°C until analysis.

After fixation and staining, images of each well were captured using ImageXpress (Molecular Devices) (Huang et al., 2011). All images were captured using ×20 Plan Apo lens. Images were captured with the FITC (ex. 490, em. 525) and Texas Red (ex. 590, em. 617) filter sets. Sixteen images were captured at the centre of each well. A total of three plates were screened to acquire three replicates for each knockdown condition. The "Cell Scoring" function from the MetaXpress software was used to calculate the number of LCVs in each channel per image. LCVs were defined as having a pixel intensity of at least 50 Gy levels above background, with a minimum width of six pixels and a maximum width of 12 pixels. LCVs were scored as disrupted if the pixel intensity in the FITC channel overlapped with the pixel intensity in the Texas Red channel. The number of disrupted LCVs in each well were recorded and analysed in Microsoft Excel. Raw data from each experimental well were normalised to the average of the negative control wells. Statistical analyses were performed on normalised data by unpaired *t* test (*$p < .05$).

4.5 | Nucleofection

Frozen differentiated BMDMs were recovered and plated at a density of 5×10^6 cells in a 10 cm dish (Falcon) in RPMI medium containing 10% (vol/vol) FBS and 10% (vol/vol) L-cell conditioned supernatant. The next day, cells were lifted in cold PBS (Gibco) and resuspended in RPMI medium containing FBS (Swanson & Isberg, 1995). Resuspended cells were aliquoted into 1.5 ml microfuge tubes at 1×10^6 cells per tube and pelleted by centrifugations for 10 min at 200*g*. Cell pellets were resuspended in nucleofector buffer (Amaxa Mouse Macrophage Nucleofector Kit [Lonza]) and 2 μg of siRNA was added to each tube (Dharmacon). Cells were transferred to a cuvette and nucleofected in the Nucleofector 2b Device (Lonza) under Y-001 program settings. Nucleofected macrophages were immediately recovered in RPMI medium containing 10% FBS and 10% L-cell supernatant. Cells were plated in 8-well chamber slides (Millipore Sigma) for microscopy assays or in 12-well plates (Corning) to prepare extracts for immunoblotting.

4.6 | Immunoblotting

Efficiency of siRNA silencing in nucleofected cells was determined by immunoblot. Nucleofected macrophages were plated in 12-well plates in RPMI medium containing 10% (vol/vol) FBS and 10% (vol/vol) L-cell supernatant. After 48 hr, cells were lysed using ×4 SDS Laemmli sample buffer (Bio-Rad) and boiled for 5 min. After fractionation on SDS-

polyacrylamide gels (Bio-Rad), proteins were transferred to nitrocellulose membranes, blocked in 4% (vol/vol) milk in TBST 0.05 M Tris-buffered saline (NaCl = 0.138 M, KCl = 0.0027 M); (Tween-20 = 0.05%, pH 8.0) (Sigma-Aldrich) and probed with antibodies to Rab5A (Cell Signalling, 1:500), Rab5B (Santa Cruz Biotechnology, 1:500), Rab5C (Novus Biologicals, 1:500), Rab11A (Cell Signalling, 1:500), Rab11B (Cell Signalling, 1:500), Rab8A (Cell Signalling Technologies, 1:500), Rab8B (Proteintech, 1:500), EEA1 (BD Biosciences, 1:500), Rab11FIP1 (Cell Signalling, 1:500), VAMP3 (Synaptic Systems, 1:500) or GAPDH (Santa Cruz Biotechnology, 1:1000) in 4% milk/TBST. Immunoblotting with primary antibodies was carried overnight at 4°C. After washing in TBST, secondary antibodies Dylight anti-rabbit IgG 680, Dylight anti-mouse IgG 680, Dylight anti-rabbit IgG 800 and Dylight anti-mouse IgG 800 (Cell Signalling 1:20,000) were incubated in 4% milk/TBST for 45 minutes at room temperature. Capture and analysis was performed using the Odyssey Scanner and the Image Studio software (LI-COR Biosciences).

4.7 | Vacuole integrity and intracellular replication assays

For fluorescence microscopy experiments, nucleofected BMDMs were seeded in 8-well chamber slides (Millipore Sigma) at a density of 5×10^4 cells per well in RPMI medium containing 10% (vol/vol) FBS and 10% (vol/vol) L-cell supernatant. After 48 hr, the medium was changed to RPMI containing 10% FBS only. Nucleofected macrophages were challenged with post-exponential phase *L. pneumophila* strains at a MOI = 1. At 1 hr after challenge, extracellular bacteria were removed by washing in PBS, and at the indicated times, macrophages were fixed with 4% (vol/vol) paraformaldehyde in PBS and blocked in PBS containing 4% BSA overnight at 4°C.

For detection of *L. pneumophila* disrupted vacuoles, nucleofected BMDMs were incubated with rabbit anti-*L. pneumophila* antisera (1:20,000) for 1 hr at 37°C in PBS containing 4% BSA followed by anti-rabbit IgG Alex Fluor 488 (Invitrogen, 1:500) for 1 hr at 37°C in PBS containing 4% BSA. After washing three times in room temperature PBS, cells were permeabilised with ice-cold methanol for 20 s, blocked in PBS containing 4% BSA for 25 min at room temperature and incubated again with *L. pneumophila* antisera (1:20,000) in PBS containing 4% BSA for 1 hr at 37°C, followed by anti-rabbit IgG Alex Fluor 594 (Invitrogen, 1:500) for 1 hr at 37°C in PBS containing 4% BSA. Disrupted vacuoles were identified by the simultaneous staining of bacteria with both Alexa Fluor 488 (bacteria detected prior to permeabilisation) and Alexa Fluor 594 (bacteria detected after permeabilisation) antibodies by fluorescence microscopy. For analysis of *L. pneumophila* intracellular replication at a single-cell level, nucleofected BMDMs were permeabilised with ice-cold methanol for 20 s, blocked in 4% BSA for 25 min at room temperature and then incubated with anti-*L. pneumophila* sera (1:20,000) for 1 hr at 37°C, followed by anti-rabbit IgG Alex Fluor 488 (1:500) for 1 hr at 37°C. The number of bacteria contained in each vacuole was quantified by fluorescence microscopy (Creasey & Isberg, 2012).

4.8 | Localisation of EEA1 or Rab11FIP1 at the *Legionella* vacuole

For EEA1 or Rab11FIP1 localisation studies, BMDMs were challenged with *L. pneumophila* strains in 8-well chamber slides. After 4 hr of incubation, cells were fixed with 4% paraformaldehyde in PBS and blocked in PBS containing 4% BSA for 1 hr at room temperature. For EEA1 staining, cells were incubated overnight at 4°C with anti-mouse EEA1 antibody (BD Biosciences, 1:50) in PBS containing 4% BSA. The next day, cells were incubated with anti-mouse IgG Alexa Fluor 488 (Invitrogen, 1:500) for 1 hr at 37°C in PBS containing 4% BSA. Cells were incubated with rabbit anti-*L. pneumophila* (1:20,000) for 1 hr at 37°C in PBS containing 4% BSA, followed by anti-rabbit IgG Dylight 405 (Invitrogen, 1:200) for 1 hr at 37°C in PBS containing 4% BSA. Cells were permeabilised with ice-cold methanol for 20 s, blocked in PBS containing 4% BSA for 25 min at room temperature, and incubated with rat anti-SidC antibody (1:200) for 1 hr at 37°C in PBS containing 4% BSA, followed by anti-rat IgG Alex Fluor 594 antibody (Invitrogen, 1:200) in PBS containing 4% BSA. Cells were incubated with *L. pneumophila* antisera (1:20,000) for 1 hr at 37°C in PBS containing 4% BSA, followed by anti-rabbit IgG Alex Fluor 647 (Invitrogen, 1:500) for 1 hr at 37°C in PBS containing 4% BSA. For Rab11FIP1 staining, cells were incubated overnight at 4°C with anti-rabbit Rab11FIP1 antibody (Cell Signalling Technologies) and staining procedures followed as described above. Chamber slides were mounted with ProLong Gold (Life Technologies) and imaged with a ×63 objective lens, using a Zeiss Axio Observer.Z1 (Zeiss) fluorescent microscope, an Apotome.2 (Zeiss) and an ORCA-R^2 digital CCD camera (Hamamatsu). Images were acquired under Cy5 (ex. 650, em. 665), FITC (ex. 490, em. 525), Texas Red (ex. 590, em. 617), and DAPI (ex. 346, em. 442) filter sets, and 2.5 μm z stacks were acquired per image (10 steps were imaged at 0.25 μm step size). Three replicates for each strain were imaged.

Volocity image analysis software (Quorum Technologies) was used to measure density distributions of EEA1 or Rab11FIP1 nearby the LCV. Objects were gated based on signal intensity as the following: bacteria were thresholded on Cy5 intensity, SidC was thresholded on Texas Red intensity, EEA1 or Rab11FIP1 was thresholded on FITC intensity. The bacteria and SidC gates were combined to define the LCV gate. The numbers of disrupted vacuoles were manually quantified in the DAPI channel. The number of EEA1 or Rab11FIP1 objects overlapping in the LCV gate were quantified and correlated with the number of disrupted vacuoles for each image. Each experiment contained three replicates for each *Legionella* strain, and quantification of ~30 vacuoles for each *Legionella* strain. Statistical analyses were performed on each replicate by unpaired *t* test (*$p < .05$, **$p < .01$, ***$p < .001$).

ACKNOWLEDGEMENTS

This work was supported by NIH/National Institute of Allergy and Infectious Diseases (NIAID) Training Grant T32GM07310 to I.S.A. as well as by HHMI and NIAID grant R01AI113211 to R.R.I. We thank Dr. Albert Tai from Tufts University Core Facility for technical

assistance in screens and Dr David Root of the Broad Institute for consultations regarding shRNA experiments. We thank members of the Isberg lab for review of the manuscript.

AUTHOR CONTRIBUTIONS

I.S.A., W.Y.C. and R.R.I. designed research; I.S.A. performed research; I.S.A., W.Y.C. and R.R.I. wrote the paper.

ORCID

Ralph R. Isberg https://orcid.org/0000-0002-8330-3554

REFERENCES

Aachoui, Y., Leaf, I. A., Hagar, J. A., Fontana, M. F., Campos, C. G., Zak, D. E., … Miao, E. A. (2013). Caspase-11 protects against bacteria that escape the vacuole. *Science*, *339*(6122), 975–978. https://doi.org/10.1126/science.1230751

Akoh, C. C., Lee, G. C., Liaw, Y. C., Huang, T. H., & Shaw, J. F. (2004). GDSL family of serine esterases/lipases. *Progress in Lipid Research*, *43*(6), 534–552. https://doi.org/10.1016/j.plipres.2004.09.002

Asrat, S., de Jesus, D. A., Hempstead, A. D., Ramabhadran, V., & Isberg, R. R. (2014). Bacterial pathogen manipulation of host membrane trafficking. *Annual Review of Cell and Developmental Biology*, *30*, 79–109. https://doi.org/10.1146/annurev-cellbio-100913-013439

Auerbuch, V., Golenbock, D. T., & Isberg, R. R. (2009). Innate immune recognition of *Yersinia pseudotuberculosis* type III secretion. *PLoS Pathogens*, *5*(12), e1000686. https://doi.org/10.1371/journal.ppat.1000686

Banerjee, M., Joshi, S., Zhang, J., Moncman, C. L., Yadav, S., Bouchard, B. A., … Whiteheart, S. W. (2017). Cellubrevin/vesicle-associated membrane protein-3-mediated endocytosis and trafficking regulate platelet functions. *Blood*, *130*(26), 2872–2883. https://doi.org/10.1182/blood-2017-02-768176

Berger, K. H., & Isberg, R. R. (1993). Two distinct defects in intracellular growth complemented by a single genetic locus in *Legionella pneumophila*. *Molecular Microbiology*, *7*(1), 7–19. https://doi.org/10.1111/j.1365-2958.1993.tb01092.x

Bucci, C., Lutcke, A., Steele-Mortimer, O., Olkkonen, V. M., Dupree, P., Chiariello, M., … Zerial, M. (1995). Co-operative regulation of endocytosis by three Rab5 isoforms. *FEBS Letters*, *366*(1), 65–71. https://doi.org/10.1016/0014-5793(95)00477-q

Burstein, D., Amaro, F., Zusman, T., Lifshitz, Z., Cohen, O., Gilbert, J. A., … Segal, G. (2016). Genomic analysis of 38 *Legionella* species identifies large and diverse effector repertoires. *Nature Genetics*, *48*(2), 167–175. https://doi.org/10.1038/ng.3481

Byrne, B., & Swanson, M. S. (1998). Expression of *Legionella pneumophila* virulence traits in response to growth conditions. *Infection and Immunity*, *66*(7), 3029–3034.

Casbon, A. J., Allen, L. A., Dunn, K. W., & Dinauer, M. C. (2009). Macrophage NADPH oxidase flavocytochrome B localizes to the plasma membrane and Rab11-positive recycling endosomes. *Journal of Immunology*, *182*(4), 2325–2339. https://doi.org/10.4049/jimmunol.0803476

Chen, S., Liang, M. C., Chia, J. N., Ngsee, J. K., & Ting, A. E. (2001). Rab8b and its interacting partner TRIP8b are involved in regulated secretion in AtT20 cells. *The Journal of Biological Chemistry*, *276*(16), 13209–13216. https://doi.org/10.1074/jbc.M010798200

Christoforidis, S., McBride, H. M., Burgoyne, R. D., & Zerial, M. (1999). The Rab5 effector EEA1 is a core component of endosome docking. *Nature*, *397*(6720), 621–625. https://doi.org/10.1038/17618

Chung, N., Zhang, X. D., Kreamer, A., Locco, L., Kuan, P. F., Bartz, S., … Strulovici, B. (2008). Median absolute deviation to improve hit selection for genome-scale RNAi screens. *Journal of Biomolecular Screening*, *13*(2), 149–158. https://doi.org/10.1177/1087057107312035

Coers, J., Vance, R. E., Fontana, M. F., & Dietrich, W. F. (2007). Restriction of *Legionella pneumophila* growth in macrophages requires the concerted action of cytokine and Naip5/Ipaf signalling pathways. *Cellular Microbiology*, *9*(10), 2344–2357. https://doi.org/10.1111/j.1462-5822.2007.00963.x

Creasey, E. A., & Isberg, R. R. (2012). The protein *SdhA* maintains the integrity of the *Legionella*-containing vacuole. *Proceedings of the National Academy of Sciences of the United States of America*, *109*(9), 3481–3486. https://doi.org/10.1073/pnas.1121286109

Creasey, E. A., & Isberg, R. R. (2014). Maintenance of vacuole integrity by bacterial pathogens. *Current Opinion in Microbiology*, *17*, 46–52. https://doi.org/10.1016/j.mib.2013.11.005

Cunha, B. A., Burillo, A., & Bouza, E. (2016). Legionnaires' disease. *Lancet*, *387*(10016), 376–385. https://doi.org/10.1016/S0140-6736(15)60078-2

de Jesus-Diaz, D. A., Murphy, C., Sol, A., Dorer, M., & Isberg, R. R. (2017). Host cell S phase restricts *Legionella pneumophila* intracellular replication by destabilizing the membrane-bound replication compartment. *MBio*, *8*(4), 1–18. https://doi.org/10.1128/mBio.02345-16

Derre, I., Swiss, R., & Agaisse, H. (2011). The lipid transfer protein CERT interacts with the *Chlamydia* inclusion protein IncD and participates to ER-*Chlamydia* inclusion membrane contact sites. *PLoS Pathogens*, *7*(6), e1002092. https://doi.org/10.1371/journal.ppat.1002092

Ensminger, A. W., Yassin, Y., Miron, A., & Isberg, R. R. (2012). Experimental evolution of *Legionella pneumophila* in mouse macrophages leads to strains with altered determinants of environmental survival. *PLoS Pathogens*, *8*(5), e1002731. https://doi.org/10.1371/journal.ppat.1002731

Finetti, F., Patrussi, L., Galgano, D., Cassioli, C., Perinetti, G., Pazour, G. J., & Baldari, C. T. (2015). The small GTPase Rab8 interacts with VAMP-3 to regulate the delivery of recycling T-cell receptors to the immune synapse. *Journal of Cell Science*, *128*(14), 2541–2552. https://doi.org/10.1242/jcs.171652

Flieger, A., Neumeister, B., & Cianciotto, N. P. (2002). Characterization of the gene encoding the major secreted lysophospholipase A of *Legionella pneumophila* and its role in detoxification of lysophosphatidylcholine. *Infection and Immunity*, *70*(11), 6094–6106. https://doi.org/10.1128/iai.70.11.6094-6106.2002

Franceschini, A., Szklarczyk, D., Frankild, S., Kuhn, M., Simonovic, M., Roth, A., … Jensen, L. J. (2013). STRING v9.1: Protein-protein interaction networks, with increased coverage and integration. *Nucleic Acids Research*, *41*(Database issue), D808–815. https://doi.org/10.1093/nar/gks1094

Gaspar, A. H., & Machner, M. P. (2014). VipD is a Rab5-activated phospholipase A1 that protects *Legionella pneumophila* from endosomal fusion. *Proceedings of the National Academy of Sciences of the United States of America*, *111*(12), 4560–4565. https://doi.org/10.1073/pnas.1316376111

Horgan, C. P., & McCaffrey, M. W. (2009). The dynamic Rab11-FIPs. *Biochemical Society Transactions*, *37*(5), 1032–1036. https://doi.org/10.1042/BST0371032

Horwitz, M. A., & Maxfield, F. R. (1984). *Legionella pneumophila* inhibits acidification of its phagosome in human monocytes. *The Journal of Cell Biology*, *99*(6), 1936–1943. https://doi.org/10.1083/jcb.99.6.1936

Horwitz, M. A., & Silverstein, S. C. (1980). Legionnaires' disease bacterium (legionella pneumophila) multiples intracellularly in human monocytes. *The Journal of Clinical Investigation*, *66*(3), 441–450. https://doi.org/10.1172/JCI109874

Hu, C., Hardee, D., & Minnear, F. (2007). Membrane fusion by VAMP3 and plasma membrane t-SNAREs. *Experimental Cell Research*, *313*(15), 3198–3209. https://doi.org/10.1016/j.yexcr.2007.06.008

Huang, L., Boyd, D., Amyot, W. M., Hempstead, A. D., Luo, Z. Q., O'Connor, T. J., … Isberg, R. R. (2011). The E block motif is associated with *Legionella pneumophila* translocated substrates. *Cellular Microbiology*, *13*(2), 227–245. https://doi.org/10.1111/j.1462-5822.2010.01531.x

Isberg, R. R., O'Connor, T. J., & Heidtman, M. (2009). The *Legionella pneumophila* replication vacuole: Making a cosy niche inside host cells. *Nature Reviews Microbiology*, *7*(1), 13–24. https://doi.org/10.1038/nrmicro1967

Kelly, E. E., Horgan, C. P., & McCaffrey, M. W. (2012). Rab11 proteins in health and disease. *Biochemical Society Transactions*, *40*(6), 1360–1367. https://doi.org/10.1042/BST20120157

Ku, B., Lee, K. H., Park, W. S., Yang, C. S., Ge, J., Lee, S. G., … Oh, B. H. (2012). VipD of *Legionella pneumophila* targets activated Rab5 and Rab22 to interfere with endosomal trafficking in macrophages. *PLoS Pathogens*, *8*(12), e1003082. https://doi.org/10.1371/journal.ppat.1003082

Laguna, R. K., Creasey, E. A., Li, Z., Valtz, N., & Isberg, R. R. (2006). A *Legionella pneumophila*-translocated substrate that is required for growth within macrophages and protection from host cell death. *Proceedings of the National Academy of Sciences of the United States of America*, *103*(49), 18745–18750. https://doi.org/10.1073/pnas.0609012103

Lapierre, L. A., Dorn, M. C., Zimmerman, C. F., Navarre, J., Burnette, J. O., & Goldenring, J. R. (2003). Rab11b resides in a vesicular compartment distinct from Rab11a in parietal cells and other epithelial cells. *Experimental Cell Research*, *290*(2), 322–331. https://doi.org/10.1016/s0014-4827(03)00340-9

Lindsay, A. J., & McCaffrey, M. W. (2004). The C2 domains of the class I Rab11 family of interacting proteins target recycling vesicles to the plasma membrane. *Journal of Cell Science*, *117*(19), 4365–4375. https://doi.org/10.1242/jcs.01280

Liu, B. C., Sarhan, J., Panda, A., Muendlein, H. I., Ilyukha, V., Coers, J., … Poltorak, A. (2018). Constitutive interferon maintains GBP expression required for release of bacterial components upstream of Pyroptosis and anti-DNA responses. *Cell Reports*, *24*(1), 155–168. e155. https://doi.org/10.1016/j.celrep.2018.06.012

Lucas, M., Gaspar, A. H., Pallara, C., Rojas, A. L., Fernandez-Recio, J., Machner, M. P., & Hierro, A. (2014). Structural basis for the recruitment and activation of the *Legionella* phospholipase VipD by the host GTPase Rab5. *Proceedings of the National Academy of Sciences of the United States of America*, *111*(34), E3514–3523. https://doi.org/10.1073/pnas.1405391111

Luo, Z. Q., & Isberg, R. R. (2004). Multiple substrates of the *Legionella pneumophila* dot/Icm system identified by interbacterial protein transfer. *Proceedings of the National Academy of Sciences of the United States of America*, *101*(3), 841–846. https://doi.org/10.1073/pnas.0304916101

McGourty, K., Thurston, T. L., Matthews, S. A., Pinaud, L., Mota, L. J., & Holden, D. W. (2012). *Salmonella* inhibits retrograde trafficking of mannose-6-phosphate receptors and lysosome function. *Science*, *338*(6109), 963–967. https://doi.org/10.1126/science.1227037

Mellouk, N., Weiner, A., Aulner, N., Schmitt, C., Elbaum, M., Shorte, S. L., … Enninga, J. (2014). *Shigella* subverts the host recycling compartment to rupture its vacuole. *Cell Host & Microbe*, *16*(4), 517–530. https://doi.org/10.1016/j.chom.2014.09.005

Pelegrin, P., Barroso-Gutierrez, C., & Surprenant, A. (2008). P2X7 receptor differentially couples to distinct release pathways for IL-1beta in mouse macrophage. *Journal of Immunology*, *180*(11), 7147–7157. https://doi.org/10.4049/jimmunol.180.11.7147

Pfeffer, S., & Aivazian, D. (2004). Targeting Rab GTPases to distinct membrane compartments. *Nature Reviews. Molecular Cell Biology*, *5*(11), 886–896. https://doi.org/10.1038/nrm1500

Pilla, D. M., Hagar, J. A., Haldar, A. K., Mason, A. K., Degrandi, D., Pfeffer, K., … Coers, J. (2014). Guanylate binding proteins promote caspase-11-dependent pyroptosis in response to cytoplasmic LPS. *Proceedings of the National Academy of Sciences of the United States of America*, *111*(16), 6046–6051. https://doi.org/10.1073/pnas.1321700111

Piro, A. S., Hernandez, D., Luoma, S., Feeley, E. M., Finethy, R., Yirga, A., … Coers, J. (2017). Detection of cytosolic *Shigella flexneri* via a C-terminal triple-arginine motif of GBP1 inhibits Actin-based motility. *MBio*, *8*(6), 1–16. https://doi.org/10.1128/mBio.01979-17

Ruiz-Albert, J., Yu, X. J., Beuzon, C. R., Blakey, A. N., Galyov, E. E., & Holden, D. W. (2002). Complementary activities of SseJ and SifA regulate dynamics of the *Salmonella typhimurium* vacuolar membrane. *Molecular Microbiology*, *44*(3), 645–661. https://doi.org/10.1046/j.1365-2958.2002.02912.x

Sato, T., Iwano, T., Kunii, M., Matsuda, S., Mizuguchi, R., Jung, Y., … Harada, A. (2014). Rab8a and Rab8b are essential for several apical transport pathways but insufficient for ciliogenesis. *Journal of Cell Science*, *127*(2), 422–431. https://doi.org/10.1242/jcs.136903

Segal, G., Feldman, M., & Zusman, T. (2005). The Icm/dot type-IV secretion systems of *Legionella pneumophila* and *Coxiella burnetii*. *FEMS Microbiology Reviews*, *29*(1), 65–81. https://doi.org/10.1016/j.femsre.2004.07.001

Shi, J., Zhao, Y., Wang, K., Shi, X., Wang, Y., Huang, H., … Shao, F. (2015). Cleavage of GSDMD by inflammatory caspases determines pyroptotic cell death. *Nature*, *526*(7575), 660–665. https://doi.org/10.1038/nature15514

Stenmark, H. (2009). Rab GTPases as coordinators of vesicle traffic. *Nature Reviews. Molecular Cell Biology*, *10*(8), 513–525. https://doi.org/10.1038/nrm2728

Swanson, M. S., & Isberg, R. R. (1995). Association of *Legionella pneumophila* with the macrophage endoplasmic reticulum. *Infection and Immunity*, *63*(9), 3609–3620.

Weber, S. S., Ragaz, C., Reus, K., Nyfeler, Y., & Hilbi, H. (2006). *Legionella pneumophila* exploits PI(4)P to anchor secreted effector proteins to the replicative vacuole. *PLoS Pathogens*, *2*(5), e46. https://doi.org/10.1371/journal.ppat.0020046

Weiner, A., Mellouk, N., Lopez-Montero, N., Chang, Y. Y., Souque, C., Schmitt, C., & Enninga, J. (2016). Macropinosomes are key players in early *Shigella* invasion and vacuolar escape in epithelial cells. *PLoS Pathogens*, *12*(5), e1005602. https://doi.org/10.1371/journal.ppat.1005602

Welz, T., Wellbourne-Wood, J., & Kerkhoff, E. (2014). Orchestration of cell surface proteins by Rab11. *Trends in Cell Biology*, *24*(7), 407–415. https://doi.org/10.1016/j.tcb.2014.02.004

Wiater, L. A., Dunn, K., Maxfield, F. R., & Shuman, H. A. (1998). Early events in phagosome establishment are required for intracellular survival of *Legionella pneumophila*. *Infection and Immunity*, *66*(9), 4450–4460.

Wilcke, M., Johannes, L., Galli, T., Mayau, V., Goud, B., & Salamero, J. (2000). Rab11 regulates the compartmentalization of early endosomes required for efficient transport from early endosomes to the trans-golgi network. *The Journal of Cell Biology*, *151*(6), 1207–1220. https://doi.org/10.1083/jcb.151.6.1207

SUPPORTING INFORMATION

Additional supporting information may be found online in the Supporting Information section at the end of this article.

How to cite this article: Anand IS, Choi W, Isberg RR. Components of the endocytic and recycling trafficking pathways interfere with the integrity of the *Legionella*-containing vacuole. *Cellular Microbiology*. 2020;22:e13151. https://doi.org/10.1111/cmi.13151